Heliyon 10 (2024) e24492

Contents lists available at ScienceDirect

Heliyon

journal homepage: www.cell.com/heliyon

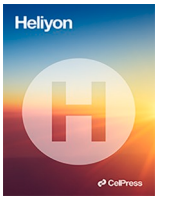

Research article

Chemically processed CdTe thin films for potential applications in solar cells – Effect of Cu doping

Azqa F. Butt [a], M. Azhar [a], Hassan Yousaf [a], K.M. Batoo [b], Dilbar Khan [a], M. Noman [a], Mujeeb U. Chaudhry [c], Shahzad Naseem [a,*], Saira Riaz [a,**]

[a] Centre of Excellence in Solid State Physics, University of the Punjab, Lahore-54590, Pakistan
[b] King Abdullah Institute For Nanotechnology, King Saud University, Riyadh-11451, Saudi Arabia
[c] Department of Engineering, Durham University, DH13LE, UK

ARTICLE INFO

Keywords:
Electrodeposition
Optical properties
Semiconductors
Thin films
CdTe

ABSTRACT

Thin films of cadmium telluride (CdTe) have attained the attention of researchers due to the potential application in solar cells. However, cost-effective fabrication of solar cells based on thin films along with remarkable efficiency and control over optical properties is still a challenging task. This study presents an analysis of the structural, optical and electrical properties of undoped and Cu-doped CdTe thin films fabricated on ITO coated glass substrates using an electrodeposition process with a focus on practical applications. Electrolytes of cadmium (Cd), tellurium (Te) and copper (Cu) are prepared with a low molarity of 0.1 M. Thin films are deposited by keeping current density in the range of 0.12–0.3 mA/cm^2. Copper doping is varied (2-10 wt%) for the optimized sample. X-ray diffraction crystallography indicates that both undoped CdTe and Cu-doped CdTe films crystallize into a dominant hexagonal lattice. Direct energy band gap is observed for both undoped and doped conditions. The study revealed a drop in the optical band gap energy to ~1.46 eV with the increase in doping (Cu) concentration from 2 to 10 wt%. Increase in mobility and conductivity is observed with the increase in current density of the deposited undoped CdTe thin films. Whereas, Cu doping of 6 wt% produced thin films with acceptable mobility and conductivity for the doped samples. Furthermore, photoluminescence (PL) spectroscopy unveiled a multitude of emission peaks encompassing the visible spectrum, arising from the combination of electrons and holes through both direct and indirect recombination processes. Findings of this study suggest that chemically produced CdTe thin films would be suitable for use as low-cost applications pertaining to solar cells.

1. Introduction

The provision of sufficient energy is one of the primary obstacles standing in the way of the nation's advancement [1]. Both renewable energy and sustainable energy are types of energy sources that are better for the environment [2,3]. Energy derived from the sun, wind, and water are all included in this category [4]. Stable, sustainable, ecologically benign source of energy can be provided by the sun to the entire world. The solar energy is readily available and the devices using this energy (solar cells) hardly require any

* Corresponding author.
** Corresponding author.
E-mail addresses: shahzad.cssp@pu.edu.pk (S. Naseem), saira_cssp@yahoo.com (S. Riaz).

https://doi.org/10.1016/j.heliyon.2024.e24492
Received 25 May 2023; Received in revised form 19 December 2023; Accepted 9 January 2024
Available online 12 January 2024

maintenance. Solar cells made of crystalline silicon hold the majority share of the market at the moment. These days, dye-sensitized solar cells [5] and thin film solar cells [6] are getting a lot of interest because of their ability to lower production costs [7,8]. The absorber layer serves as the device's central processing unit in solar cells based on thin films. It is possible to use a variety of thin films for this layer, including cadmium telluride (CdTe), thin film of silicon, gallium arsenide (GaAs), antimony sulphide (Sb_2S_3) and copper indium gallium selenide [9,10]. Despite of the CIGS low price and better efficiency, compounds with four elements are difficult to manufacture [11]. Further, the efficiency of solar cells based on thin films of amorphous silicon is currently not very high [12]. CdTe is the most desirable and promising material for the production of solar cells based on thin-films because of its low processing and production cost along with relatively high efficiency as compared to other thin films based solar cells. CdTe, commonly known as cadmium telluride, is II-VI compound semiconductor that belongs to the chalcogenide family.

Thin-film photovoltaic (PV) technology using solar energy holds great potential for the future life of mankind [13]. Due to suitable properties of CdTe including its optical type and value of energy band gap, high value of absorption coefficient, uniform growth provision using both chemical and physical methods, control over conductivity, its relatively higher theoretical conversion efficiency (33 %) [14,15] along with reasonable settlement time after investment [16,17]—it has attracted the attention of many research groups. Its strong binding energy and high melting temperature of 1041 °C [18] contribute to the stability. Polycrystalline CdTe is a flexible material even in the realm of manufacture. Solar cells [19], sensors, chemical and physical [20], diagnosting imaging [21], and detectors based on electromagnetic radiations including X-ray and gamma - ray [22] are just some of the many semiconductor devices that could benefit from this technology.

CdTe thin films have been developed using various methods, including the pulsed laser approach [23], sputtering [24], thermal evaporation [25], chemical-bath approach [26], and electrodeposition [27]. The cost of material prepared using the physical approach is high due to the need for vacuum pumps and gauges. Chemical techniques are gaining much attention among researcher's community because of their low cost and large area growth. Nevertheless, it can be challenging to manage a number of factors, including composition, purity, etc. [28]. There are benefits and drawbacks to using various deposition methods. Electrodeposition method can be chosen because of the feasibility to produce materials with n- and p-type conductivity by adjusting the deposition voltage and/or current density [29,30]. Scalability, low cost, waste reduction, simplicity, high quality, low toxic waste production, and ease of doping can be the additive advantages of electrodeposition technique. Electrodeposited materials can be prepared at room temperature and tuning the deposition parameters may allow to produce fine-grained film with uniform thickness and composition [31,32]. The absorbance of the layer in solar cell devices is proportional to the thickness of the film, which is mostly regulated by the deposition parameters [33].

In earlier studies, the efficiency of a solar cell device made of glass/FTO/CdS/CdTe/Au was tested in both dark and light conditions [34]. On the other hand, this lengthens the time it takes to process the order, which ultimately drives up the price. Doping can be used to increase the conductivity of CdTe thin films and improve its efficiency [35]. Copper can modify the photovoltaic characteristics of solar cells during the manufacturing process that can affect the performance of solar cells [34,35]. Copper can migrate from a back contact that contains copper to the cell junction. Similarly, storing a Cu-doped CdTe single crystal at ambient temperature results in a noticeable shift in its luminous characteristics [36,37]. The hole density or p-type conductivity of a CdTe layer can be improved by doping with Cu [38]. In addition, copper is one of the elements that is deliberately added to electronic devices to affect their performance. As a result, it is necessary to get an in-depth understanding of the effect that Cu can produce in CdTe material.

In this study, effects of Cu-doping are studied for CdTe thin films. Electrodeposition technique is used to prepare undoped and copper doped CdTe thin films using ITO coated glass substrates. Ethylene glycol was used as solvent and salts of cadmium and tellurium were used as precursors. The prepared samples were deposited using variation in pH and current density using electrodeposition technique. Optimized sample was selected to be doped by copper (Cu). Thin films developed in the present study offered a provision to tune the energy band gap, conductivity and mobility under undoped and doped conditions without following the complex procedure and/or post deposition treatments. The use of ethylene glycol in depositing CdTe films on indium tin oxide (ITO) coated substrates offers certain advantages that include conductivity and structural stability. Ethylene glycol serves as a solvent and stabilizer in the deposition process. The C–O and O–H groups in ethylene glycol contribute to its unique properties, promoting the formation of sigma bonds that enhance the polarity of the solution [39]. The current findings will prove to be of assistance in the production of Cu-doped CdTe-based solar cells that have high conversion efficiencies.

2. Experimental details

2.1. Materials

Research grade cadmium chloride bi hydrated, tellurium nitrate and copper chloride bi hidrated were used for synthesis of the material. De-ionized (DI) water and ethylene glycol were utilized as a solvent.

2.2. Synthesis details

Cadmium telluride thin films were deposited by cost effective electrodeposition technique on ITO coated glass substrates. An electrolyte, containing 0.1 M cadmium chloride and tellurium nitrate was prepared using 200 ml of ethylene glycol. The conductivity advantage in this context may be attributed to ethylene glycol's ability to facilitate the transport of Cd and Te ions to the substrate surface during electrodeposition. Its polar nature and solvating properties can enhance the mobility of charged species, allowing for a more efficient deposition process. Additionally, the stabilizing effect of ethylene glycol may contribute to the uniform and controlled

growth of CdTe films on the ITO-coated substrate. Overall, the use of ethylene glycol in the deposition of CdTe films on ITO-coated substrates is likely driven by its role in optimizing the electrochemical conditions for efficient film formation, resulting in improved conductivity and desirable film characteristics for electronic applications, such as solar cells [39]. Electrolytes were prepared by stirring the solution for 4 h. Molarity and pH of the electrolytes is varied and analyzed using cyclic voltammetry. pH was varied in the range of 3–7 by adding appropriate amount of sodium hydroxide. Copper chloride was separately mixed in ethylene glycol, and mixing was performed at room temperature; this solution was used as a dopant solution. Electrolytes prepared with pH 3 were selected to be used to deposit undoped and Cu doped thin films of cadmium telluride, deposition response of the Cd and Te ions with varying potential and time is shown in Fig. 1(a and b). CdTe thin films were prepared by keeping current density in the range of 0.12–0.3 mA/cm^2. Substrates were rinsed with DI water and placed in an ultrasonic bath using acetone and isopropyl alcohol for the removal of impurities. In an electrolyte, vertically positioned ITO coated glass substrate is considered as working electrode. Platinum wire was used as counter electrode, whereas saturated calomel electrode (SCE) was used as a reference electrode. Detailed steps of synthesis can be seen in Fig. 2. Thin films with dark brown-grey colored were observed at 0.2–0.3 mA/cm^2 current density, whereas, dark grey colored thin films were observed at relatively low values of current density.

2.3. Characterization techniques

For crystal structural analysis of thin films, X-ray Diffractometer was used for the angular range of $2\theta^\circ = 20–80^\circ$. 30 kV and 20 mA were used to produce Cu Kα radiations (1.5406 Å). The optical properties of films were studied by J.A. Woollam M − 2000 Variable Angle Spectroscopic Ellipsometer (VASE) and Shimadzu's UV–Vis spectrophotometer. Hall measurement setup was used to study the electrical properties of the samples. FS5 spectrofluorometer, Edinburgh Instrument, equipped with a xenon arc lamp was used for photoluminescence analysis.

3. Results and discussion

3.1. Structural results

XRD analysis was performed to assess the crystallographic growth of undoped CdTe thin films on ITO coated substrates [Fig. 3]. CdTe thin films were produced by keeping various current density values. Hexagonal dominated CdTe phase was observed in the XRD patterns [Fig. 3], whereas no peaks related to Cd and Te ions were detected. XRD peaks were labelled with (102), (013), (022), and (204) planes related to hexagonal lattice of CdTe. Less intense cubic planes were also observed under all the conditions. Increase in peaks intensity along with lower 2 theta shift was observed with the increase in current density to 0.15 mA/cm^2. This result shows that thin films were affected by tensile strain during the growth. Minimum contribution from cubic phase was observed with the increase in current density to 0.2 mA/cm^2. Slight variation in the peak position of the (013) plane might have been observed because of the strain produced due the development of cubic and hexagonal phase of CdTe. A similar scenario of mixed cubic and hexagonal phases of electrodeposited CdTe thin film deposited on FTO glass substrates grown at different deposition times was reported by Yimamu et al. [40].

Response of crystallite size, strain, stacking fault probability (SFP) and texture coefficient was calculated by Eqs. (1)–(4) [41].

$$t = \frac{0.9\,\lambda}{\beta\,cos\,\theta} \tag{1}$$

In above equation, λ stands for wavelength (1.5408 Å), β for full width at half maximum (FWHM) and θ represents Bragg angle.

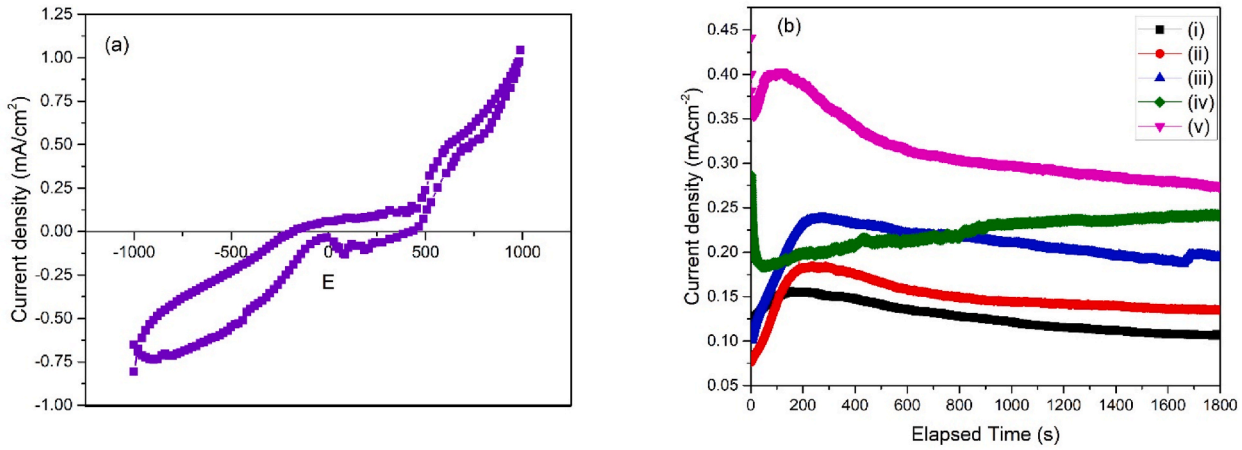

Fig. 1. (a) Cyclic voltammetry and (b) current vs. elapsed time plots for of (i–v) S1–S5.

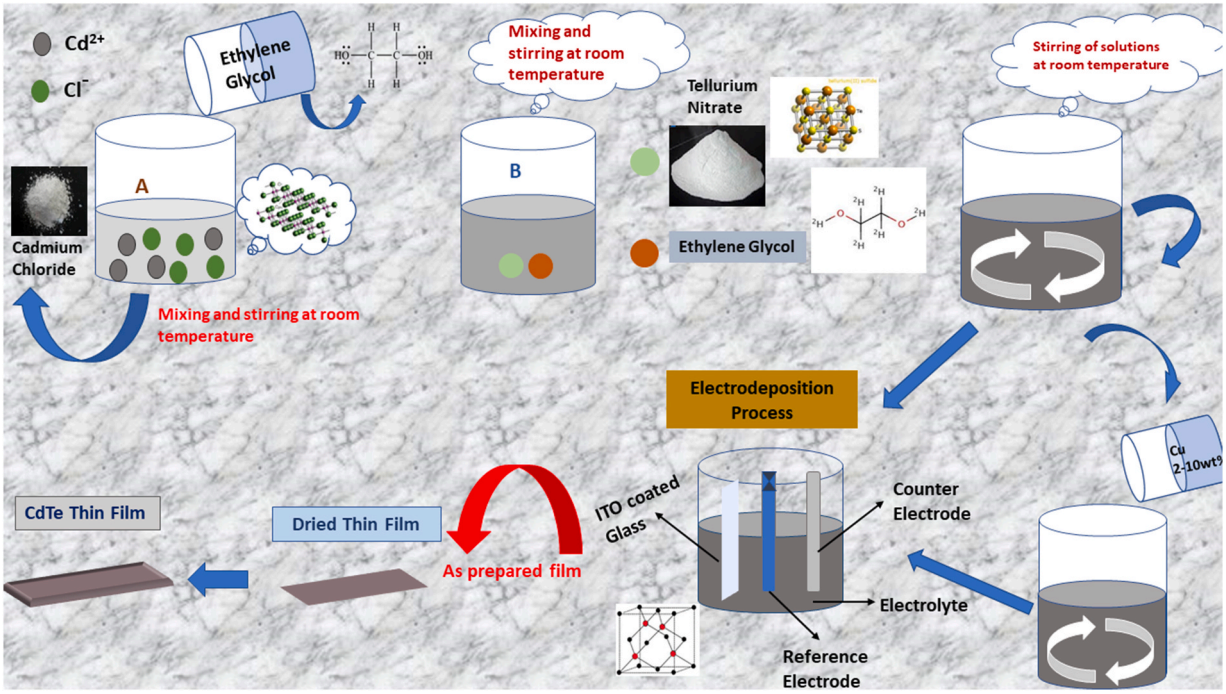

Fig. 2. Flow diagram for the preparation of thin films.

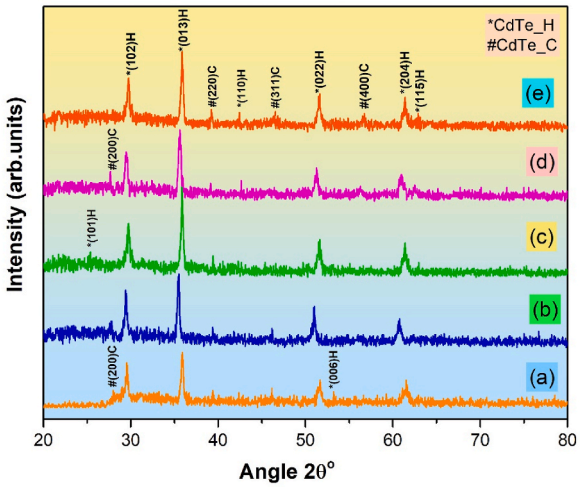

Fig. 3. XRD patterns of CdTe thin films prepared by keeping current density of (s1-S5): (a–e) 0.12–0.3 mAcm^{-2}..

Microstrain in thin films were calculated using Eq. (2) [41].

$$\text{Strain} = \varepsilon = \frac{\Delta d}{d} \tag{2}$$

The stacking fault probability can be calculated by using Eq. (3) [41].

$$\textit{Stacking Fault Probability} = \left[\frac{2\pi^2}{45\sqrt{3}tan\,\theta}\right] * \Delta 2\theta \tag{3}$$

Increase in crystallite size was witnessed with the increase in current density to 0.2 mA/cm^2 (S3). Further increase in current density led to a decreased value of crystallite size as shown in Fig. 4(a). Increased film thickness and formation of larger crystallite size may produce lower value of strain because of the reduced number of grain boundaries and defects [42]. Several factors including nucleation and growth mechanism along with the coalescence of smaller crystallites contribute to the formation of a continuous thin

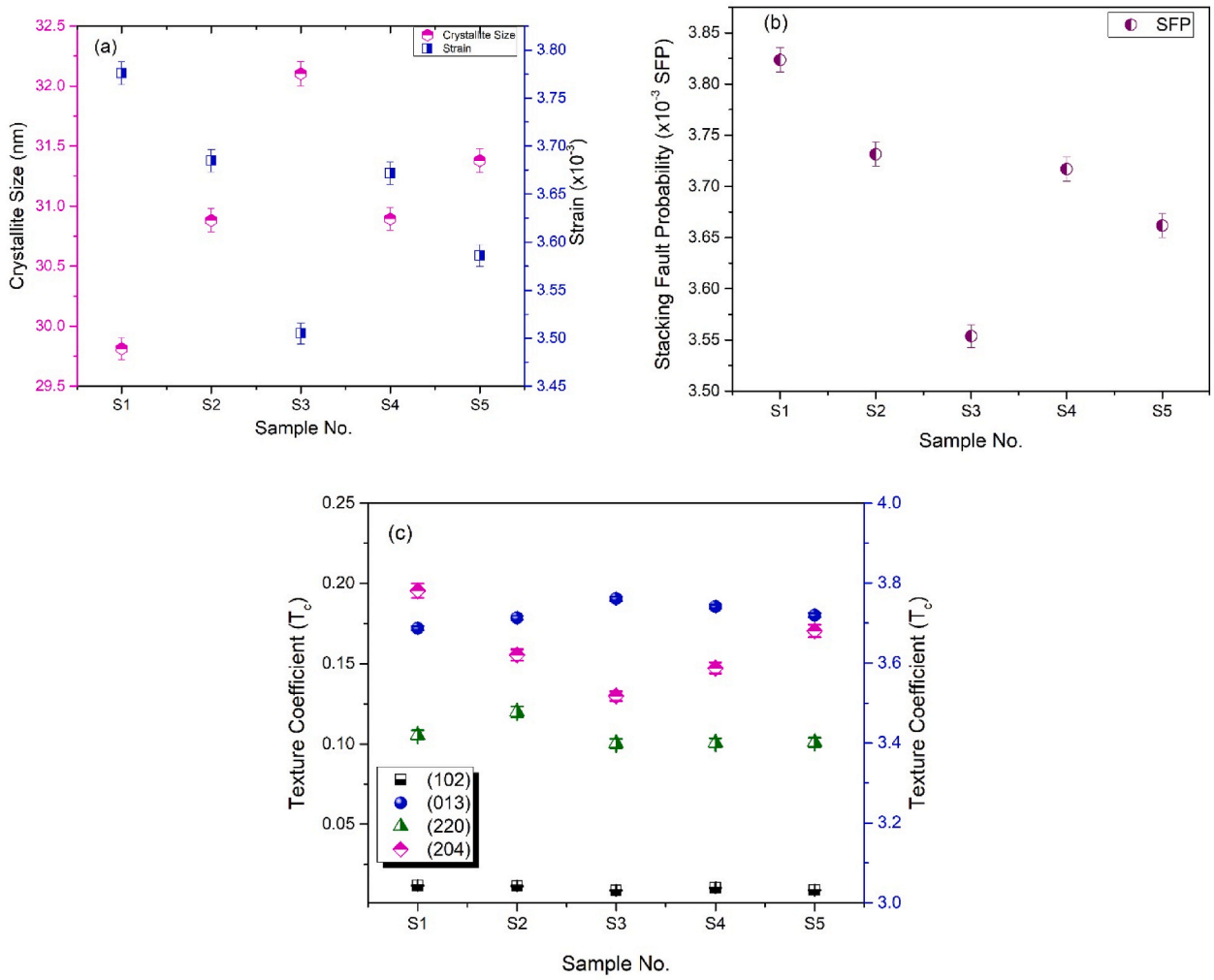

Fig. 4. Variation in (a) crystallite size & strain, (b) stacking fault probability and (c) texture coefficient by keeping current density of (S1–S5) 0.12–0.3 mAcm^{-2}..

and homogenous thin film. The probability of forming larger crystallites at particular value of current density was observed because of the enhanced electrostatic interaction [43]. Phase strengthening and stability are key parameters responsible for the growth of larger crystallites. Deposition parameters (such as temperature, pH of solution, deposition rate, electric field between counter and working electrodes, contaminants, etc.) can also introduce inherent stress into films [44]. The FWHM of the XRD peaks is affected by a number of different parameters, including strain, crystallite size, inhomogeneous distribution of particle size, and experimental broadening [44]. As can be seen in Fig. 4(a), the formation of dominant hexagonal phase of CdTe at current density of 0.2 mA/cm^2 led to minimum development of strain in thin film. As can be shown in Fig. 4(b), the dominant hexagonal phase of CdTe (S3) produced reduced value of stacking fault probability (SFP).

The changes in texture coefficient was also estimated by following formula as shown in Eq. (4) [41].

$$T_c = \frac{\frac{I_{(hkl)}}{I_{0(hkl)}}}{\left(\frac{1}{N}\right)\sum\left[\frac{I_{(hkl)}}{I_{0(hkl)}}\right]} \tag{4}$$

$I_{(hkl)}$ stands for intensity of (hkl) planes observed from XRD patterns, $I_{o(hkl)}$ shows intensity obtained from standard data, N = number of diffraction peaks.

Polycrystalline thin films have a unique property known as a preferred crystal orientation, which could have an impact on the film's optical, electrical, and magnetic properties. Structural re-arrangement may lead to shift in preferred orientation. Texture coefficient values can be used to identify if a thin film has undergone a shift towards a more random crystal orientation or vice versa. Fig. 4(c) shows variation in texture coefficient for CdTe thin films. Minimized structural stresses and surface energy may lead to a dominant preferred orientation along a specific plane [45,46].

The structural characterization of the doped CdTe thin films prepared by keeping current density of 0.2 mA/cm^2 is shown in Fig. 5. Copper (Cu) doping was varied in the range of 2 to 10 wt%. All the films were found to have a polycrystalline structure, as evidenced by the presence of reflection lines corresponding to the (102), (013), (220), and (204) diffraction planes, which is consistent with the presence of the hexagonal phase of CdTe structure (ICSD 01-080-0088). It is important to note that the XRD patterns did not exhibit any additional metallic peak linked to copper phases, such as copper oxide and/or copper cluster. This is evidence that Cu^{2+} ions were successfully incorporated into the CdTe lattice without causing a change in the hexagonal structure of CdTe. It was observed through Fig. 5(b) that the peak location of the (013) plane is moved towards higher diffraction angles as a result of the strain caused in the film by the inclusion of Cu ions in the CdTe structure [47]. Increase in crystallinity was observed with the increase in doping content to 6 wt %, this is evident with the increased intensity of the crystal planes [Fig. 5(a-c)]. Thin films of Zn- and Cu-doped CdTe were reported to exhibit the similar behaviour in the literature [48,49]. Decreased peak intensity was observed with the further increase in doping content to 8–10 wt% as shown in Fig. 5(d and e).

Variations in crystallite size and strain of CdTe thin films as a function of dopant concentration (2-10 wt%) is shown in Fig. 6 (a). It was determined that the value of the average crystallite size of the Cu-doped CdTe film varies from ~25 to 36 nm. The intensity of (013) plane was increased when the Cu doping percentage was increased to 6 wt%. Increased crystallite size along with decreased value of strain and stacking fault probability was observed with the increase in doping content to 6 wt% [Fig. 6(a-b)]. Further increase in doping led to a relative decrease in crystallite size and increase in the values of strain and stacking fault probability. This doping dependent behaviour describes the incorporation of Cu^{2+} ions into the CdTe lattice that helped to enhance the crystallinity and decreased defects for the thin films prepared with 6 wt% doping, similar response has been reported previously [50]. The incorporation of Cu ions, with 2 wt% doping into the CdTe thin films, led to increased value of strain as compared to the undped thin films. However, reduced strain values were observed with the increase in doping content to 6 wt% as compared to the undoped CdTe thin films. Dopant concentration may have strong effect on the crystallite size, surface morphology and orientation of crystal lattices [51,52]. Variation in texture coefficient is shown in Fig. 6 (c).

3.2. Optical studies

UV–Vis spectroscopy was used to examine the absorbance spectra [Fig. 7 (a,b)] and energy band gap values [Fig. 8] of the undoped and Cu-doped CdTe thin films. UV–Vis spectra of the CdTe thin films, under doped and undoped, demonstrated that the CdTe thin films have a high optical absorbance. Absorption coefficient was calculated using Beer-Lambert's law as given below in Eqs. (5) and (6) [53]:

$$-log_{10}\frac{I}{I_o} = \alpha.d \tag{5}$$

Or

$$I = I_o e^{-\alpha d} \tag{6}$$

where I is the intensity that is being transmitted, I_o is the intensity that is being incident onto the film, d is the thickness.

Higher absorbance values can be attributed to the increased crystallite size and reduced defects. It has been observed that the thin films, doped and undoped, exhibited significant absorbance in the near visible range, that can help in the improved performance of the CdTe absorber layer for solar cell. The introduction of a Cu dopant into a CdTe lattice caused a reorganization of the bonds and a shift in the local structure of CdTe, i.e. dominant hexagonal to single hexagonal phase as shown in Figs. 3 and 5.

Direct optical band gap (E_g) of undoped and Cu doped CdTe thin films, i.e. inter band transition between conduction and valence

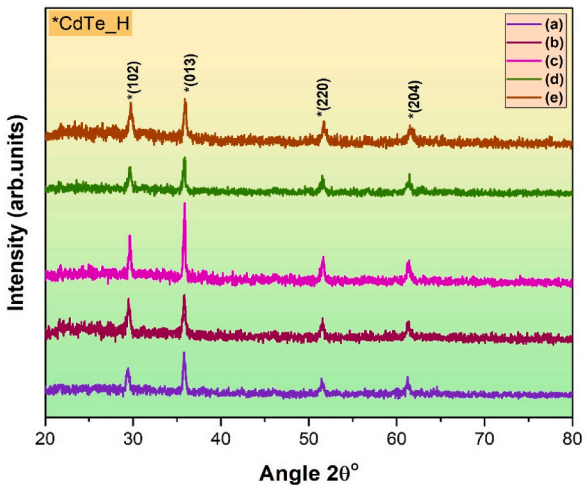

Fig. 5. XRD patterns of Cu doped CdTe thin films prepared with varying dopant concentration of (a–e)2-10 wt%.

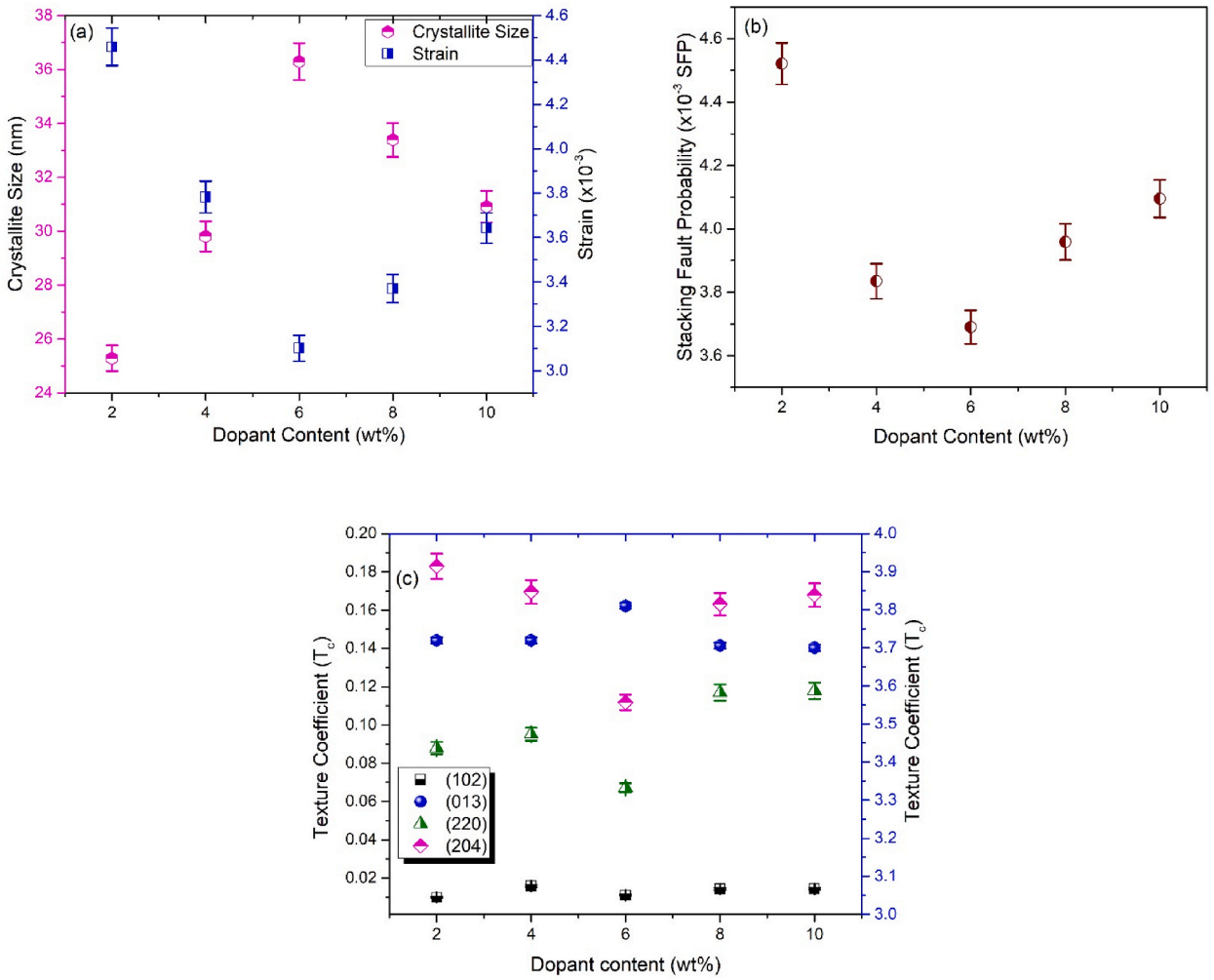

Fig. 6. Variation in (a) crystallite size & strain, (b) stacking fault probability and (c) texture coefficient for copper doped CdTe thin films.

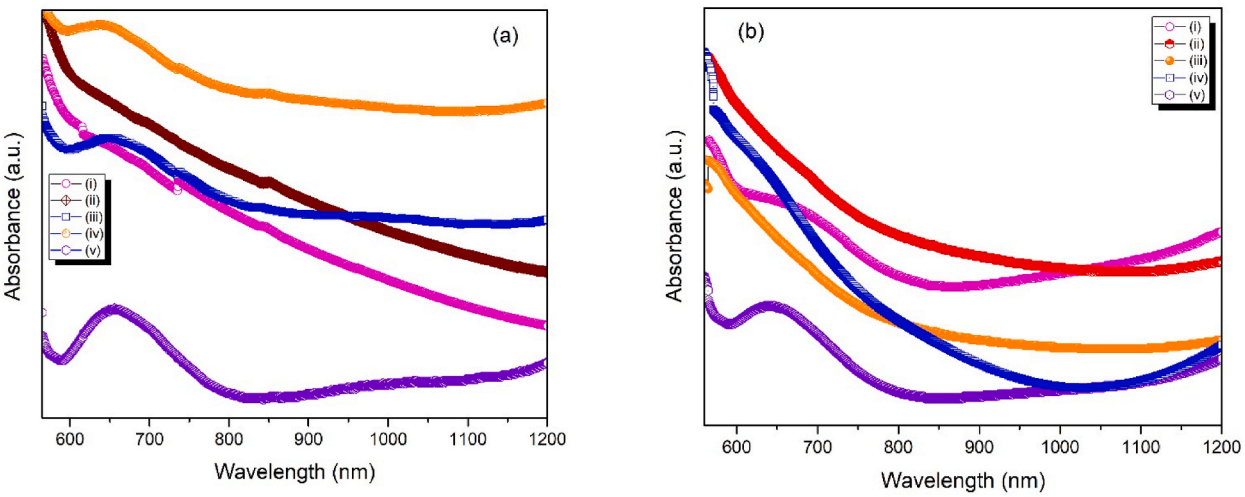

Fig. 7. Absorbance spectra of (a) undoped CdTe (i–v: S1–S5) and (b) Cu doped (i–v: 2-10 wt%) CdTe thin Films.

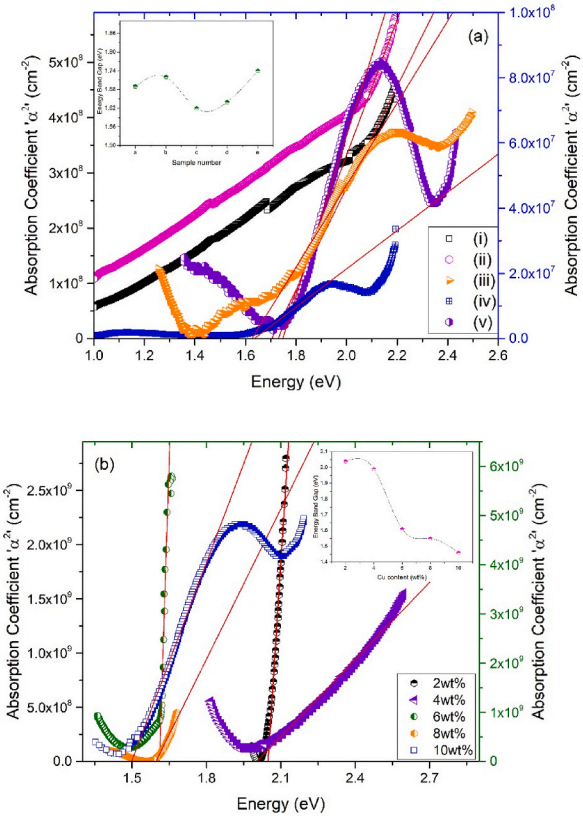

Fig. 8. Absorption coefficient for (a) undoped (i-v:S1–S5) and (b) Cu doped CdTe thin films.

band, can be calculated using Tauc Eq. (7) [54].

$$(\alpha_{h\nu}) = A\ (h\nu - E_g)^{1/2} \tag{7}$$

Where A is constant; α is absorption coefficient; hν is photon energy; E_g is optical band gap.

Fig. 8(a and b) illustrates the variation in direct energy band gap values of undoped and Cu doped CdTe thin films. Undoped CdTe thin films exhibited band gap values in the range of ~1.62–1.74 eV. Minimum value of 1.62 eV was observed for the samples S3. Cu doped samples were prepared with particular value of current density and by varying Cu content from 2 to 10 wt%. Direct band gap values in the range of ~1.46–2.04 eV were observed for Cu doped CdTe thin films. CdTe thin films prepared with Cu doping content of 2-4 wt% exhibited higher value of band gap, i.e. ~2 eV. Decrease in the energy band gap values to 1.6 eV was observed with the increase in doping content to 6 wt%. Further, decrease in band gap values to 1.55–1.46 eV was observed with the increase in doping content to 8-10 wt%.

Relatively higher band gap values for undoped CdTe thin films and thin films prepared with 2-4 wt% Cu doping was observed in the present study. Burstein–Moss (BM) effect can be used to explain bandgap widening, the valence band becomes significantly emptied because of higher carrier concentration and the highest energy states in the valence band are blocked [55], this phenomenon has been corelated with the variation in conductivity and carrier concentration values that will be discussed in the later section of electrical results. Many-body effect of free carriers on the conduction and valence bands, can be used to explain bandgap narrowing (BGN) and is known as bandgap renormalization [56]. A blue shift, can be observed because of of higher hole concentration, the "Burstein-Moss" shift, whereas a red shift is caused by the band gap renormalization. The band gap shifts depend on material, the type of doping and the carrier concentration [57].

Thin film and material characterization tool known as spectroscopic ellipsometry (SE) is based on the change in amplitude (recorded in the parameter ψ, psi) and phase (Δ, delta) of polarized light reflecting from a surface. This change in amplitude is what gives spectroscopic ellipsometry (SE) its name. Typically, the values of ψ and Δ are influenced by the wavelength of the incident light used for investigating a material, along with the optical characteristics, thicknesses, and surface roughness of the film. The experimental data were obtained at an incidence angle of 70°. In order to determine the thickness of the film, the Cauchy model was utilized. The software makes use of three optical layer models (the Cauchy layer of the substrate, the layer of film, and the surface roughness layer) in order to determine the film thickness. The experimental and fitted data of ψ and Δ versus wavelength for a thin layer of CdTe on an ITO coated glass substrate are depicted in Fig. 9(a–e) and 10 (a-e).

Variable-Angle Spectroscopic Ellipsometer was used to evaluate the refractive index (n) and extinction coefficient (k). Cauchy

model was used for fitting the experimentally observed data. The variation in values of refractive index (n) and extinction coefficient (k) of undoped and Cu doped CdTe thin films are shown in Fig. 11(a–d). There are several parameters including porosity, defects as well as phase purity that may affect refractive index of thin films. High refractive index ~2.33 at 700 nm, for undoped thin films, is due to higher optical density [58,59]. Increase in refractive index was observed with the increase in doping content.

The electronic polarizability and the local electrical field inside the materials are two of the most essential components that

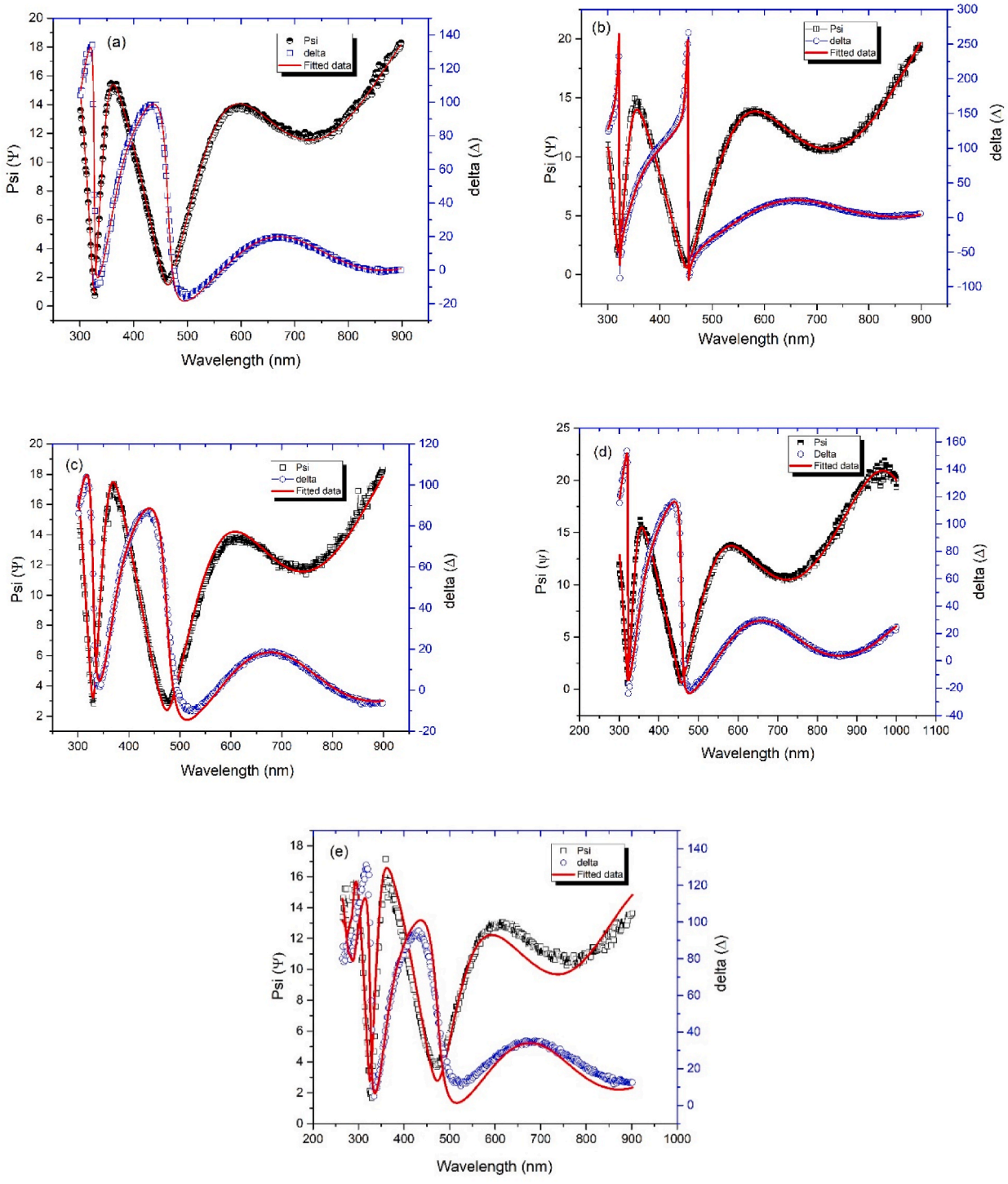

Fig. 9. Variation in ellipsometry data (Ψ and Δ) for undoped CdTe thin films (a–e: S1–S5, with variation in current density).

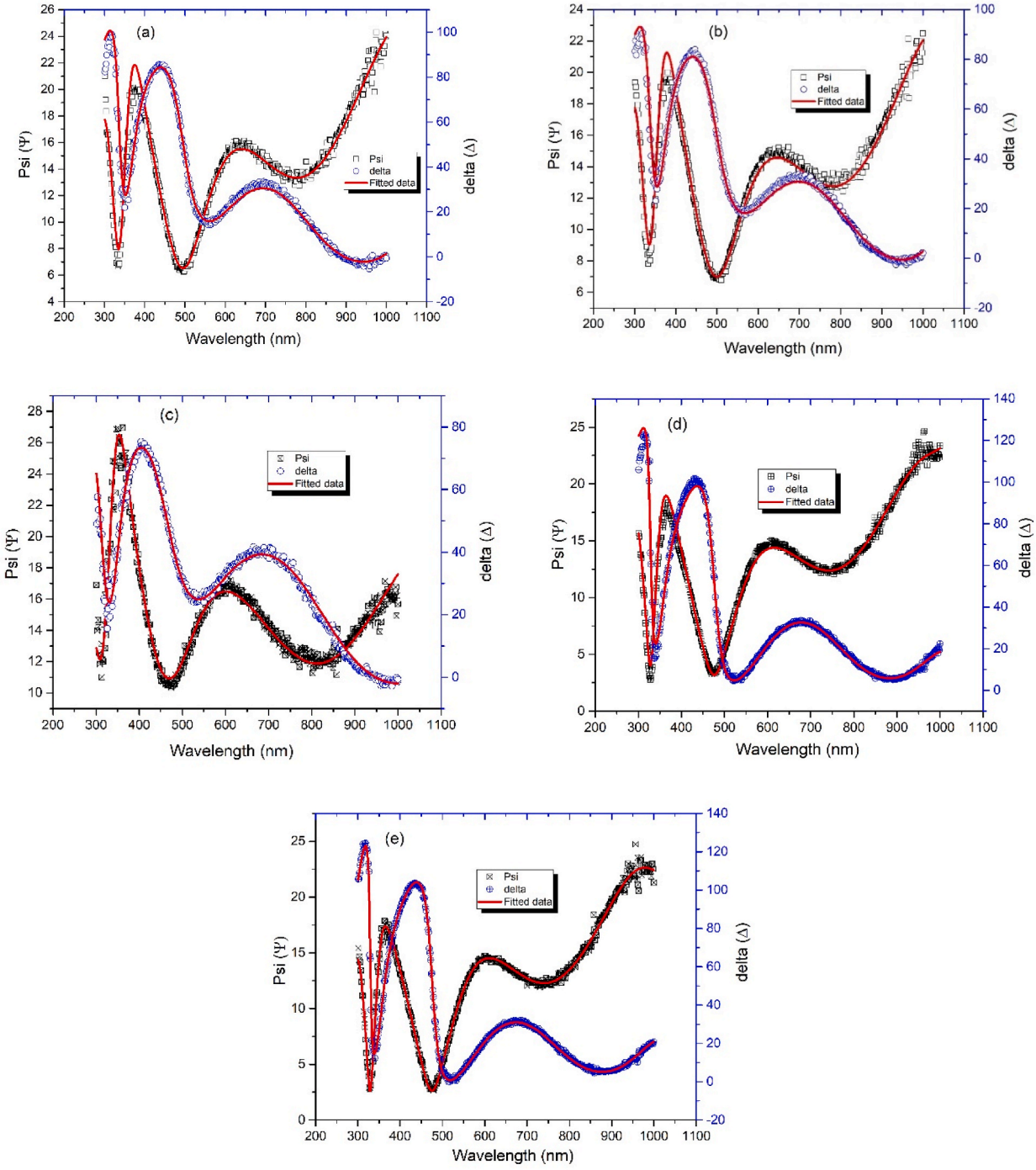

Fig. 10. Variation in ellipsometry data (Ψ and Δ) for Cu doped CdTe thin films (a–e: 2-10 wt% doping content).

determine the refractive index (n) of the thin film [60]. The extinction coefficient (k) measures the amount of light that is absorbed through the material. The amount of light that is absorbed by a particular substance at a certain wavelength is proportional to either its mass density or its carrier concentration [58,61].

Optical dielectric constant, real (ε_1) and imaginary (ε_2), of undoped and Cu doped CdTe thin films were calculated using following Eqs. (8) and (9) [54].

$$\varepsilon_1 = n^2 - k^2 \tag{8}$$

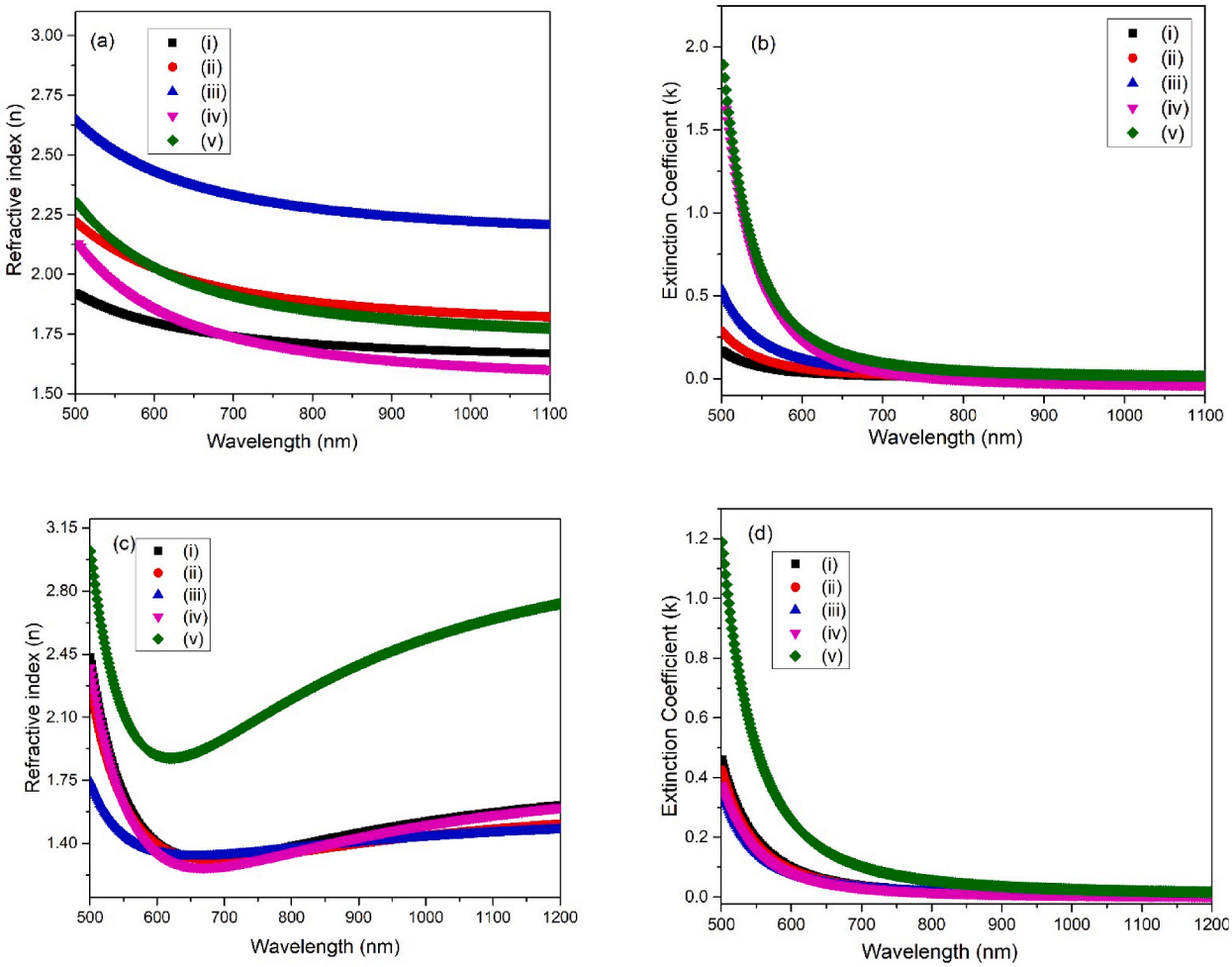

Fig. 11. (a) Refractive index, (b) extinction coefficient, for undoped (i–v: S1–S5) and (c) refractive index, (d) extinction coefficient for Cu doped CdTe thin films (i–v: 2-10 wt%).

$$\varepsilon_2 = 2nk \tag{9}$$

ε_1 is maximum energy that material can store and ε_2 depicts absorption of electrical energy and is known as relative loss factor. Values of ε_1 and ε_2 decrease with wavelength and come to be constant at relatively higher wavelengths as shown in Fig. 12(a–d).

3.3. Analysis of photoluminescence (PL) emission

To analyze the deposited samples' PL characteristics, an FS5 spectrofluorometer equipped with a xenon arc lamp was used. The use of photoluminescence as a method for verifying the presence of electronic transitions in semiconductor materials is an effective approach. Determining the precise energy levels of nanostructures or polycrystalline thin films is a fundamental process that photoluminescence spectroscopy assists with. Fig. 13 presents an analysis of the PL spectra of thin films of undoped and Cu doped CdTe. Density of trap states are dependent on the synthesis and deposition parameters [62].

The PL spectra of undoped CdTe films exhibit a sharp and narrow emission peak at 598 nm for S3 sample using excitation wavelength of 395 nm, that is closely associated with the normal energy band gap of an undoped CdTe thin film. There is a decrease in emission wavelength on either side of the sample S3. These variations can be easily correlated with the traps and extra energy levels due to the lattice mismatch and structural defects, as shown in section 3.1. The CdTe sample of lower quality exhibits defect bands at 757 nm and 778 nm that possesses the size-dependent energy level shift induced by the changing of quantum confinement effect [62–65]. This provides evidence that the deep center defect band can be utilized to monitor the surface quality of the substrate and is associated with native defects that are connected to growth and processing, such as interstitials and vacancies. Multiple transitions may be present, according to the shape of the wide 500 nm-800 nm region [63,64,66]. The shoulder peaks of samples S1 and S2 at 468 nm and 479 nm occurs as a consequence of the recombination of excited electrons that become trapped at shallow levels, thereby producing bound electron–hole pairs [62,64].

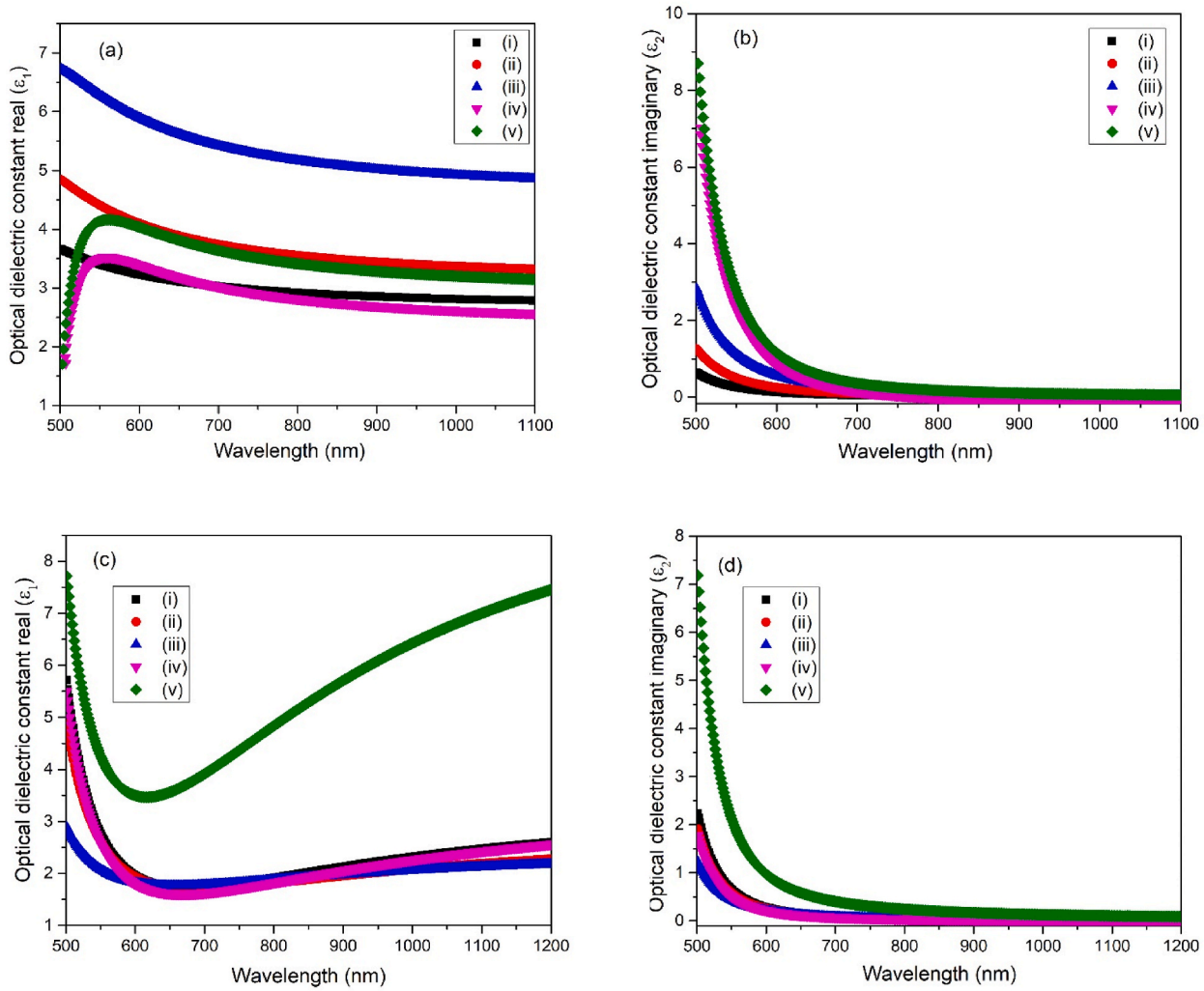

Fig. 12. Variation in (a) optical dielectric constant real, (b) optical dielectric constant imaginary for undoped (i–v: S1–S5) and in (c) optical dielectric constant real, (d) optical dielectric constant imaginary for Cu doped CdTe thin films (i–v:2-10 wt%).

The 2 % copper doping in sample S3 exhibits a PL peak at a lower wavelength as compared to the undoped sample [Fig. 13 (b)] because of the extra holes/carriers generated due to the doping effect. This is equivalent to a larger band gap as given by Burstein-Moss effect [55,67]. Further addition of copper content (6–10 %) adds trapping levels in the band gap thus producing an effect that is equivalent to a reduction in the effective band gap values. It is possible that the emission peak that corresponds to 557 nm and 561 nm is caused by structural defects that are present in the films as a result of lattice mismatch [68]. On the other hand, this peak is attributed to the radiative carrier recombination process that occurs during the transition from one band to another [66,69]. The intensity of the PL peak is found to vary with the concentration of Cu in CdTe films. It is noticed that films with 6 wt% Cu concentration exhibited a higher peak intensity at 567 nm. This observation can be attributed to the improved crystalline quality and reduced presence of crystallographic defects [68,63,64,70], as previously mentioned in the XRD analysis. Additionally, films doped with 6 wt% Cu showed reduced lattice variations as indicated by a higher PL peak intensity. When it comes to PL spectra, the key parameters that are considered are the intensity, the line edge, and the full width at half maximum (FWHM). A higher intensity implies a low defect density, while a greater FWHM suggests a poor crystalline structure, and vice versa. In accordance to this, peaks with broader FWHM with low intensity at 578 nm and 585 nm depicted the defects/traps due to poor crystallinity. These results correlate well with the results shown in the optical analyses taken by the UV–Vis spectrophotometer as given in section 3.2.

3.4. Electrical studies

The Hall effect measurements were utilized to explore the type and concentration of charge carriers as well as the Hall mobility (H) for undoped CdTe and Cu doped CdTe thin films. The findings of this investigation are shown in Fig. 14. Increased value of mobility with decreased carrier concentration led to increased value of conductivity for the undoped thin films prepared with the variation in

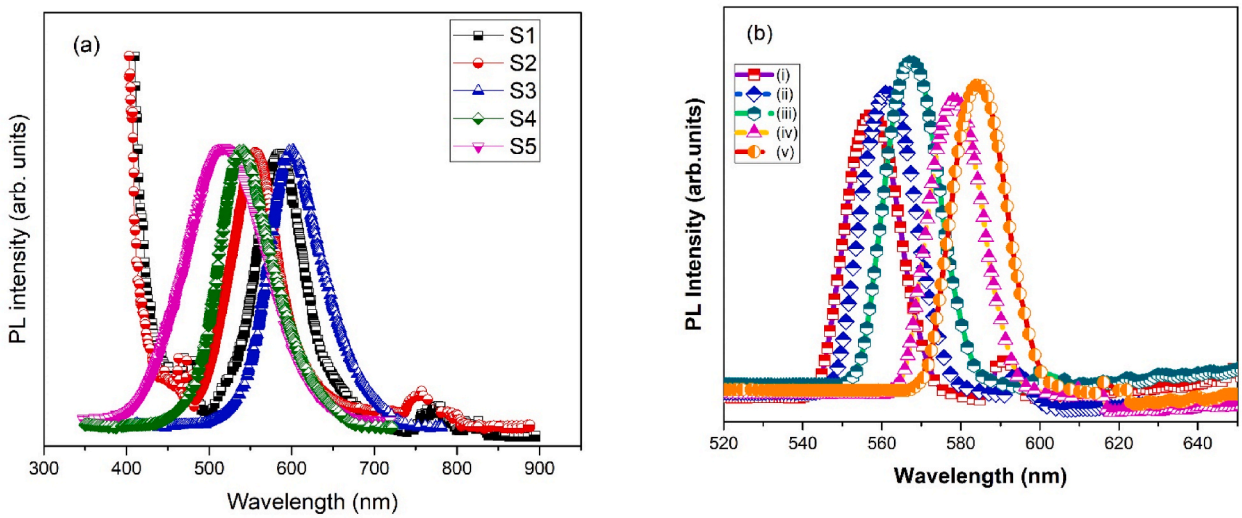

Fig. 13. The photoluminescence spectra of (a) undoped CdTe thin films (S1–S5) and (b) copper doped CdTe thin films (i–v):2-10 wt%.

current density as shown in Fig. 14(a and b). Increased values of carrier concentration and conductivity was observed for the Cu doped thin films [Fig. 14 (c-d)] as compared to the undoped films. The built-in-potential in the CdTe-absorber-layer region is increased by a large concentration of acceptor carriers [71]. Cu doping has produced significant effect on the mobility of the samples. This is a result of the decreased/increased scattering of the carrier from the surface, the elimination of defects in the films, and the increased crystalline structure that results from the decreased number of grain boundaries. Our research demonstrated that both undoped and Cu doped CdTe have room temperature resistivities in the range of 2–25 Ω-cm for undoped CdTe thin films, whereas 0.5 – 5.7 Ω-cm for Cu doped CdTe thin films. Niraula et al. [72] found analogous results for undoped CdTe films of 0.5 μm thickness produced by MOCVD in the 423–573 K temperature range. The same was true for thermally evaporated CdTe thin films at RT with thicknesses of 0.3–0.5 μm and 0.5 μm by Rusu et al. [73] and Nory [74], respectively. Though, the findings of earlier studies [75] indicated lower values than then reported. This disparity could be explained by the fact that the methods of preparation and the conditions under which the film was deposited are different. It has been reported previously that synthesis and preparation methods/parameters can affect the transport of charge carriers [76].

4. Conclusions

Electrodeposition, being an application-oriented method, was used to prepare undoped and Cu-doped CdTe thin films on ITO coated glass substrates. pH of the electrolyte was varied as 3–7. Undoped CdTe thin films were prepared by keeping current density in the range of 0.12–0.3 mA/cm^2. Copper doped CdTe thin films were prepared by varying doping concentration in the range of 2-10 wt% at particular current density. The XRD investigation showed the formation of dominant hexagonal CdTe phase for undoped thin films. Whereas, Cu doping in CdTe led to the formation of hexagonal CdTe lattice under all the doping conditions. Increased crystallite size and decreased strain values were observed for the thin films prepared with 6 wt% Cu doping. The optical direct energy band gap of undoped CdTe varied from 1.62 to 1.74 eV. Lower value of energy band gap (1.46 eV) was observed for the thin film prepared with Cu doping. These results were correlated with the carrier concentration, mobility and conductivity of undoped and doped samples. Photoluminescence (PL) spectroscopy exhibited several emission peaks within the visible spectrum, arising from electron-hole recombination both directly and indirectly. It is possible to draw the conclusion that an increase in conductivity coincides with an increase in the Cu incorporation level as compared to the undoped thin films, which in turn can be beneficial for its potential use an absorber layer in solar cells.

Data availability statement

All relevant data has been used in the manuscript.

CRediT authorship contribution statement

Azqa F. Butt: Writing – original draft. **M. Azhar:** Methodology. **Hassan Yousaf:** Formal analysis. **K.M. Batoo:** Formal analysis. **Dilbar Khan:** Formal analysis. **M. Noman:** Methodology. **Mujeeb U. Chaudhry:** Investigation. **Shahzad Naseem:** Visualization, Supervision, Resources, Conceptualization. **Saira Riaz:** Writing – review & editing, Visualization, Supervision, Conceptualization.

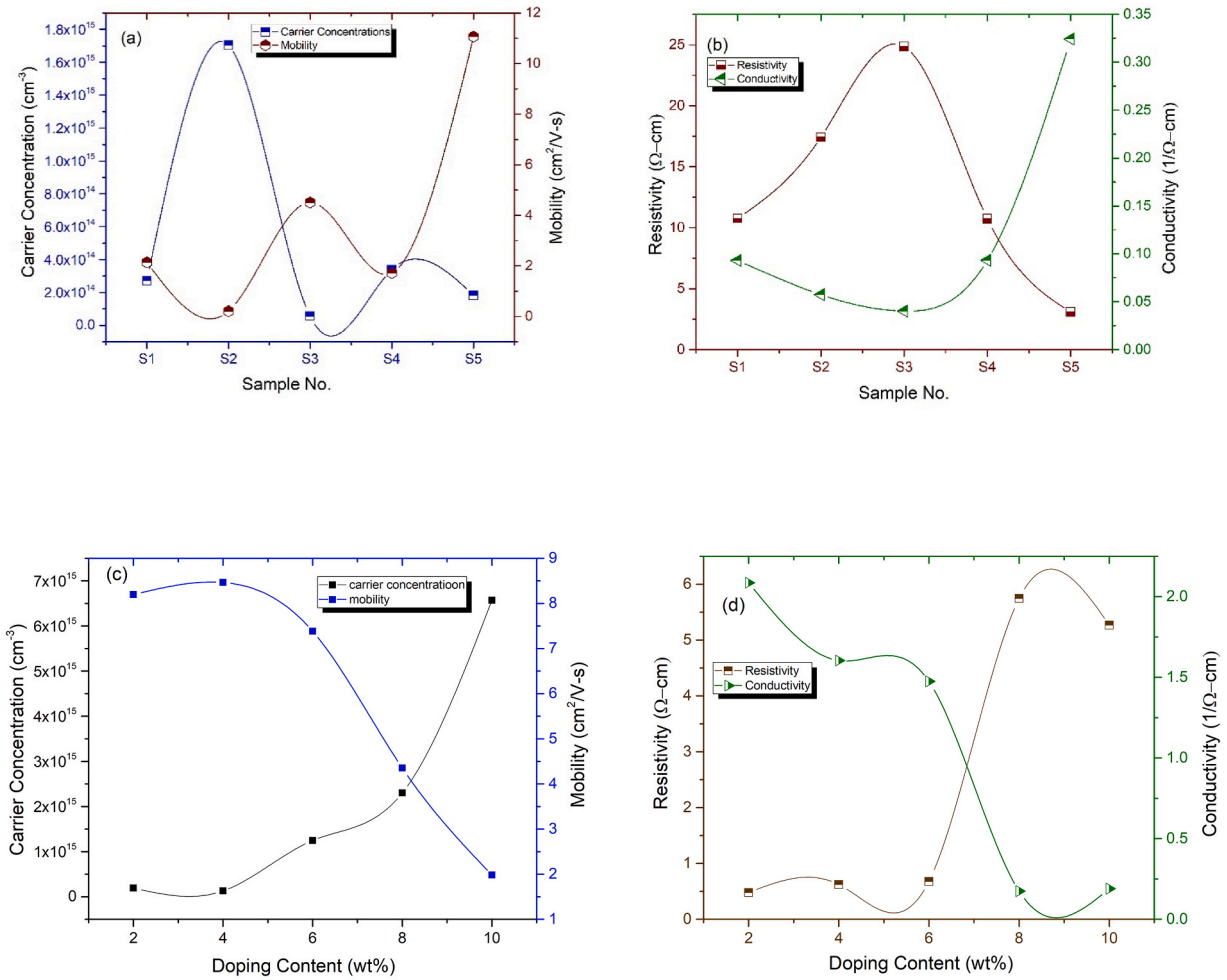

Fig. 14. Variation in (a) carrier concentration & mobility, (b) resistivity & conductivity for undoped CdTe thin films, whereas (c) carrier concentration & mobility, (d) resistivity & conductivity for Cu doped CdTe thin films.

Declaration of competing interest

The authors declare that they have no known competing financial interests or personal relationships that could have appeared to influence the work reported in this paper.

Acknowledgments

The authors are thankful to Higher Education Commission and Punjab University for the financial support. The authors would like to thank Researchers Supporting Project No. (RSP2024R148) at King Saud University, Riyadh, Saudi Arabia.

References

[1] X. Zhang, Y. Tang, F. Zhang, C. Lee, A novel aluminum-graphite dual-ion battery, Adv. Energy Mater. 6 (11) (2016) 1502588.
[2] M. Wang, C. Jiang, S. Zhang, X. Song, Y. Tang, H. Cheng, Reversible calcium alloying enables a practical room-temperature rechargeable calcium-ion battery with a high discharge voltage, Nat. Chem. 10 (6) (2018) 667–672.
[3] X. Feng, L. Sun, W. Wang, Y. Zhao, J. Shi, Construction of CdS@ZnO core–shell nanorod arrays by atomic layer deposition for efficient photoelectrochemical H_2 evolution, Separ. Purif. Technol. 324 (2023) 124520.
[4] S. Sarker, M.T. Islam, A. Rauf, H. Al Jame, S. Ahsan, M.S. Islam, M.R. Jani, S.S. Nishat, K.M. Shorowordi, S. Ahmed, A simulation based incremental study of stable perovskite-on-perovskite tandem solar device utilizing non-toxic tin and germanium perovskite, Mater. Today Commun. 32 (2022) 103881.
[5] J. Zhang, A. Zhong, G. Huang, M. Yang, D. Li, M. Teng, D. Han, Enhanced efficiency with CDCA co-adsorption for dye-sensitized solar cells based on metallosalophen complexes, Sol. Energy 209 (2020) 316–324.
[6] X. Li, S. Aftab, A. Abbas, S. Hussain, M. Aslam, F. Kabir, H.S. Abd-Rabboh, H.H. Hegazy, F. Xu, M.Z. Ansari, Advances in mixed 2D and 3D perovskite heterostructure solar cells: a comprehensive review, Nano Energy 118 (2023) 108979.
[7] W. Moloto, P.J. Mafa, P. Mbule, E. Nxumalo, B. Ntsendwana, Photoinduced electrochemical effect of porous BiPOM on TiO_2 photoanode performance for dye-sensitized solar cells application, Mater. Today Commun. 30 (2022) 103001.

[8] V. Rondán-Gómez, I. Montoya De Los Santos, D. Seuret-Jiménez, F. Ayala-Mató, A. Zamudio-Lara, T. Robles-Bonilla, M. Courel, Recent advances in dye-sensitized solar cells, Appl. Phys. A 125 (2019) 1–24.
[9] Y. Yun, S. Moon, S. Kim, J. Lee, Flexible fabric-based GaAs thin-film solar cell for wearable energy harvesting applications, Sol. Energy Mater. Sol. Cell. 246 (2022) 111930.
[10] X. Wang, R. Tang, C. Wu, C. Zhu, T. Chen, Development of antimony sulfide–selenide Sb2 (S, Se) 3-based solar cells, J. Energy Chem. 27 (3) (2018) 713–721.
[11] S. Sharma, K.K. Jain, A. Sharma, Solar cells: in research and applications—a review, Mater. Sci. Appl. 6 (12) (2015) 1145.
[12] M. Imamzai, M. Aghaei, Y.H.M. Thayoob, M. Forouzanfar, A review on comparison between traditional silicon solar cells and thin-film CdTe solar cells, in: In Proceedings of National Graduate Conference, Nat-Grad, 2012, November, pp. 1–5.
[13] V. Benda, Photovoltaics, including new technologies (Thin film) and a discussion on module efficiency, in: Future Energy, 2020, pp. 375–412.
[14] S.S. Oluyamo, A.A. Faremi, O.I.O. Olusola, Y.A. Odusote, Tunability of conductivity type and energy band gap of CdTe thin film in the electrodeposition technique, Mater. Today: Proc. 38 (2021) 558–563.
[15] A. Morales-Acevedo, Thin film CdS/CdTe solar cells: research perspectives, Sol. Energy 80 (6) (2006) 675–681.
[16] A.H. Munshi, N. Sasidharan, S. Pinkayan, K.L. Barth, W.S. Sampath, W. Ongsakul, Thin-film CdTe photovoltaics–The technology for utility scale sustainable energy generation, Sol. Energy 173 (2018) 511–516.
[17] V.M. Fthenakis, H.C. Kim, CdTe photovoltaics: life cycle environmental profile and comparisons, Thin Solid Films 515 (15) (2007) 5961–5963.
[18] A. Bosio, N. Romeo, S. Mazzamuto, V. Canevari, Polycrystalline CdTe thin films for photovoltaic applications, Prog. Cryst. Growth Char. Mater. 52 (4) (2006) 247–279.
[19] A.G. Aberle, Thin-film solar cells, Thin Solid Films 517 (17) (2009) 4706–4710.
[20] B. Ai, Z. Fan, Z.J. Wong, Plasmonic–perovskite solar cells, light emitters, and sensors, Microsystems & Nanoengineering 8 (1) (2022) 5.
[21] W.R. Hendee, E.R. Ritenour, Medical Imaging Physics, John Wiley & Sons, 2003.
[22] C. Szeles, CdZnTe and CdTe materials for X-ray and gamma ray radiation detector applications, Phys. Status Solidi 241 (3) (2004) 783–790.
[23] D. Wang, Y. Yang, T. Guo, X. Xiong, Y. Xie, K. Li, M. Ghali, Effect of pulse bias voltages on performance of CdTe thin film solar cells prepared by pulsed laser deposition, Sol. Energy 213 (2021) 118–125.
[24] H. Wang, L. Zhang, C. Ding, M. Ali, H. Qi, F. Wang, W. Sun, Ultrafast nonlinear optical properties of Ag-CdTe thin films by co-sputtering in the near-infrared region, Opt. Mater. 142 (2023) 114062.
[25] R.K.K.G.R.G. Kumarasinghe, P.K.K. Kumarasinghe, R.P. Wijesundera, B.S. Dassanayake, Thermally evaporated CdS/CdTe thin film solar cells: optimization of CdCl2 evaporation treatment on absorber layer, Curr. Appl. Phys. 33 (2022) 33–40.
[26] S. Surabhi, S. Rajpal, S.R. Kumar, A new route for preparing CdTe thin films by chemical bath deposition, Mater. Today: Proc. 44 (2021) 1463–1467.
[27] A.U. Yimamu, M.A. Afrassa, B.F. Dejene, K.G. Tshabalala, S.Z. Werta, J.J. Terblans, S.J. Motloung, The effect of growth voltage on the structure, electrical and optical properties of CdTe thin films prepared by electrodeposition method, Harla Journal of Applied Science and Materials 1 (1) (2022) 46–56.
[28] R. Smith, Chemical Process: Design and Integration, John Wiley & Sons, 2005.
[29] F. Xiao, C. Hangarter, B. Yoo, Y. Rheem, K.H. Lee, N.V. Myung, Recent progress in electrodeposition of thermoelectric thin films and nanostructures, Electrochim. Acta 53 (28) (2008) 8103–8117.
[30] O.I. Olusola, M.L. Madugu, N.A. Abdul-Manaf, I.M. Dharmadasa, Growth and characterisation of n-and p-type ZnTe thin films for applications in electronic devices, Curr. Appl. Phys. 16 (2) (2016) 120–130.
[31] E. Pellicer, A. Varea, S. Pané, K.M. Sivaraman, B.J. Nelson, S. Suriñach, M.D. Baró, J. Sort, A comparison between fine-grained and nanocrystalline electrodeposited Cu–Ni films. Insights on mechanical and corrosion performance, Surf. Coating. Technol. 205 (23–24) (2011) 5285–5293.
[32] C.J. Hibberd, E. Chassaing, W. Liu, D.B. Mitzi, D. Lincot, A.N. Tiwari, Non-vacuum methods for formation of Cu (In, Ga)(Se, S) 2 thin film photovoltaic absorbers, Prog. Photovoltaics Res. Appl. 18 (6) (2010) 434–452.
[33] M.A. Hossain, B.A. Merzougui, F.H. Alharbi, N. Tabet, Electrochemical deposition of bulk MoS2 thin films for photovoltaic applications, Sol. Energy Mater. Sol. Cell. 186 (2018) 165–174.
[34] I.M. Dharmadasa, A.A. Ojo, Unravelling complex nature of CdS/CdTe based thin film solar cells, J. Mater. Sci. Mater. Electron. 28 (2017) 16598–16617.
[35] G.H. Tariq, M. Anis-ur-Rehman, Annealing effects on physical properties of doped CdTe thin films for photovoltaic applications, Mater. Sci. Semicond. Process. 30 (2015) 665–671.
[36] T.D. Dzhafarov, S.S. Yesilkaya, N.Y. Canli, M. Caliskan, Diffusion and influence of Cu on properties of CdTe thin films and CdTe/CdS cells, Sol. Energy Mater. Sol. Cell. 85 (3) (2005) 371–383.
[37] 1. Perrenoud, L. Kranz, C. Gretener, F. Pianezzi, S. Nishiwaki, S. Buecheler, A.N. Tiwari, A comprehensive picture of Cu doping in CdTe solar cells, J. Appl. Phys. 114 (17) (2013).
[38] K.K. Chin, T.A. Gessert, S.H. Wei, The roles of CU impurity states in CdTe thin film solar cells, in: 2010 35th IEEE Photovoltaic Specialists Conference, IEEE, 2010, June, pp. 1915–1918.
[39] M. Schlesinger, M. Paunovic (Eds.), Modern Electroplating, vol. 52, John Wiley & Sons, 2014.
[40] A.U. Yimamu, M.A. Afrassa, B.F. Dejene, O.K. Echendu, K.G. Tshabalala, J.J. Terblans, H.C. Swart, S.J. Motloung, Influence of growth time on the properties of CdTe thin films grown by electrodeposition using acetate precursor for solar energy application, Mater. Res. Express 10 (5) (2023) 056403.
[41] B.D. Cullity, Elements of X-Ray Diffraction, Addison-Wesley Publishing, 1956.
[42] E.J.A.M. Arzt, Size effects in materials due to microstructural and dimensional constraints: a comparative review, Acta Mater. 46 (16) (1998) 5611–5626.
[43] J.P. Lommerse, A.J. Stone, R. Taylor, F.H. Allen, The nature and geometry of intermolecular interactions between halogens and oxygen or nitrogen, J. Am. Chem. Soc. 118 (13) (1996) 3108–3116.
[44] L. Besra, M. Liu, A review on fundamentals and applications of electrophoretic deposition (EPD), Prog. Mater. Sci. 52 (1) (2007) 1–61.
[45] J.P. Zhao, X. Wang, Z.Y. Chen, S.Q. Yang, T.S. Shi, X.H. Liu, Overall energy model for preferred growth of TiN films during filtered arc deposition, J. Phys. Appl. Phys. 30 (1) (1997) 5.
[46] M. Waqas, S. Niaz, K.M. Batoo, S. Khalid, S. Atiq, Y.B. Xu, S. Naseem, S. Riaz, Robust ferromagnetism and magneto-dielectric anomalies in (Al, Cr) co-doped iron oxide thin films-microwave mediated sol–gel approach, J. Mater. Res. Technol. 26 (2023) 6636–6651.
[47] M. Alzaid, N.M.A. Hadia, M. El-Hagary, E.R. Shaaban, W.S. Mohamed, Microstructural, optical, and electrical characteristics of Cu-doped CdTe nanocrystalline films for designing absorber layer in solar cell applications, J. Mater. Sci. Mater. Electron. 32 (11) (2021) 15095–15107.
[48] M.A. Sayeed, H.K. Rouf, Effect of Zn-doping on the structural, optical and electrical properties of thermally vacuum evaporated CdTe thin films, Surface. Interfac. 23 (2021) 100968.
[49] M. Thangaraju, A. Jayaram, R. Kandasamy, Structural, morphological, optical and electrical properties of e-beam deposited nanocrystalline CdTe: Cu alloy thin films from mechanical alloyed samples, Appl. Surf. Sci. 449 (2018) 2–9.
[50] A. Goktas, Role of simultaneous substitution of Cu^{2+} and Mn^{2+} in ZnS thin films: defects-induced enhanced room temperature ferromagnetism and photoluminescence, Phys. E Low-dimens. Syst. Nanostruct. 117 (2020) 113828.
[51] L.G. Devi, N. Kottam, S.G. Kumar, Preparation and characterization of Mn-doped titanates with a bicrystalline framework: correlation of the crystallite size with the synergistic effect on the photocatalytic activity, J. Phys. Chem. C 113 (35) (2009) 15593–15601.
[52] P. Monisha, P. Priyadharshini, S.S. Gomathi, K. Pushpanathan, Influence of Mn dopant on the crystallite size, optical and magnetic behaviour of CoFe2O4 magnetic nanoparticles, J. Phys. Chem. Solid. 148 (2021) 109654.
[53] D.F. Swinehart, The beer-lambert law, J. Chem. Educ. 39 (7) (1962) 333.
[54] M. Fox, Optical Properties of Solids, 2002.
[55] A.A. Ziabari, S.M. Rozati, Carrier transport and bandgap shift in n-type degenerate ZnO thin films: the effect of band edge nonparabolicity, Phys. B Condens. Matter 407 (23) (2012) 4512–4517.

[56] C.E. Kim, P. Moon, S. Kim, J.M. Myoung, H.W. Jang, J. Bang, I. Yun, Effect of carrier concentration on optical bandgap shift in ZnO: Ga thin films, Thin Solid Films 518 (22) (2010) 6304–6307.
[57] S. Bharadwaj, S.M. Islam, K. Nomoto, V. Protasenko, A. Chaney, H.G. Xing, D. Jena, Bandgap narrowing and Mott transition in Si-doped Al0. 7Ga0. 3N, Appl. Phys. Lett. 114 (11) (2019).
[58] S. Saha, U. Pal, A.K. Chaudhuri, V.V. Rao, H.D. Banerjee, Optical properties of CdTe thin films, Phys. Status Solidi 114 (2) (1989) 721–729.
[59] H.H. Perkampus, UV-VIS Spectroscopy and its Applications, Springer Science & Business Media, 2013.
[60] A.S. Hassanien, Studies on dielectric properties, opto-electrical parameters and electronic polarizability of thermally evaporated amorphous Cd50S50− xSex thin films, J. Alloys Compd. 671 (2016) 566–578.
[61] J. Mistrik, S. Kasap, H.E. Ruda, C. Koughia, J. Singh, Optical Properties of Electronic Materials: Fundamentals and Characterization, Springer handbook of electronic and photonic materials, 2017, 1-1.
[62] C. Karkera, G.R. Dillip, S.W. Joo, D. Kekuda, Heterogeneity of photoluminescence properties and electronic transitions in copper oxide thin films: a thickness dependent structural and optical study, Ceram. Int. 44 (14) (2018) 16984–16991.
[63] J.A. Garcia-Monge, C.D. Vazquez-Colon, A. Ponce, G. Guisbiers, A.A. Ayon, Synergistic photoluminescent interaction of Si and CdTe quantum dots 28 (2022) 1497–1504.
[64] E. Elibol, P.S. Elibol, M. Çadırcı, N. Tutkun, Improved photoluminescence and monodisperse performance of colloidal CdTe quantum dots with Cannula method, Korean J. Chem. Eng. 36 (4) (2019) 625–634.
[65] X. Mathew, J.R. Arizmendi, J. Campos, P.J. Sebastian, N.R. Mathews, C.R. Jimenez, M.G. Jimenez, R. Silva-Gonzalez, M.E. Hernandez-Torres, R. Dhere, Shallow levels in the band gap of CdTe films deposited on metallic substrates 70 (2001) 379–393.
[66] R. Furstenberg, J.O. White, Photoluminescence study of the 1.3–1.55 eV defect band in CdTe, J. Cryst. Growth 305 (1) (2007) 228–236.
[67] D.S. Ginley, J.D. Perkins, Transparent conductors, in: Handbook of Transparent Conductors, Springer US, Boston, MA, 2010, pp. 1–25.
[68] Z.R. Khan, M. Zulfequar, M.S. Khan, Structural, optical, photoluminescence, dielectric and electrical studies of vacuum-evaporated CdTe thin films, Bull. Mater. Sci. 35 (2012) 169–174.
[69] J. Zázvorka, P. Hlídek, R. Grill, J. Franc, E. Belas, Photoluminescence of CdTe: in the spectral range around 1.1 eV, J. Lumin. 177 (2016) 71–81.
[70] H. Zhang, B. Xie, X. Meng, U. Müller, B. Yilmaz, M. Feyen, S. Maurer, H. Gies, T. Tatsumi, F.S. Xiao, Rational synthesis of Beta zeolite with improved quality by decreasing crystallization temperature in organotemplate-free route, Microporous Mesoporous Mater. 180 (2013) 123–129.
[71] G. Kartopu, O. Oklobia, D. Turkay, D.R. Diercks, B.P. Gorman, V. Barrioz, S. Campbell, J.D. Major, M.K. Al Turkestani, S. Yerci, T.M. Barnes, N.S. Beattie, G. Zoppi, S. Jones, S.J.C. Irvine, Study of thin film poly-crystalline CdTe solar cells presenting high acceptor concentrations achieved by in-situ arsenic doping, Sol. Energy Mater. Sol. Cell. 194 (2019) 259–267.
[72] M. Niraula, T. Aoki, Y. Nakanishi, Y. Hatanaka, Radical assisted metalorganic chemical vapor deposition of CdTe on GaAs and carrier transport mechanism in CdTe/n-GaAs heterojunction, J. Appl. Phys. 83 (5) (1998) 2656–2661.
[73] G.G. Rusu, M. Rusu, E.K. Polychroniadis, C. Lioutas, Characterization of CdTe thin films prepared by stacked layer method, J. Optoelectron. Adv. Mater. 7 (4) (2005) 1957–1964.
[74] E.M. Nory, Investigation of Optical and Electrical Properties of Se/CdTe Heterojunction, Doctoral dissertation, Ph. D. thesis, University of Baghdad, College of Science, Baghdad, Iraq, 2008.
[75] G.G. Rusu, On the electrical and optical properties of nanocrystalline CdTe thin films, J. Optoelectron. Adv. Mater. 3 (4) (2001) 861–866.
[76] S. Du, J. Yin, H. Xie, Y. Sun, T. Fang, Y. Wang, R. Zheng, Auger scattering dynamic of photo-excited hot carriers in nano-graphite film, Appl. Phys. Lett. 121 (18) (2022) 181104.